Intramolecular relaxation observed in the surface of the quasi-one-dimensional organic conductor β-(BEDT-TTF)$_2$PF$_6$

Masahiko Ishida,[1,*] Osamu Takeuchi,[1] Takehiko Mori,[2] and Hidemi Shigekawa[1,†]
[1]*Institute of Applied Physics, CREST, Japan Science and Technology Corporation (JST), University of Tsukuba, Tsukuba 305-8573, Japan*
[2]*Department of Organic and Polymeric Materials, Tokyo Institute of Technology, Tokyo 152-8552, Japan*
(Received 11 May 2001; published 18 September 2001)

In addition to the intermolecular symmetry breaking which is generally observed during the surface relaxation/reconstruction of atomic crystals, intramolecular relaxation is expected to exist in the case of molecular crystals, which was confirmed on the surface of β-(BEDT-TTF)$_2$PF$_6$ [BEDT-TTF is bis(ethylenedithio)tetrathiafulvalene] by using scanning tunneling microscopy (STM). Two types of molecular images obtained by STM were comprehensively explained by the spatial distributions of the highest-occupied molecular orbital calculated for the two types of the molecular structures. One is the structure appearing in the crystal that is derived from the x-ray diffraction measurement, which was used in the previous calculations to reproduce the STM images. The other is the relaxed molecular structure calculated by optimization of the molecular structure.

DOI: 10.1103/PhysRevB.64.153405 PACS number(s): 68.35.Bs, 68.37.Ef, 61.66.Hq

On the surface of materials, crystal symmetry breaks in order to stabilize the surface structure by reducing the surface energy.[1–5] Generally, the total energy of the ideal surfaces is increased by the occurrence of chemical bond breaking, and great changes such as atomic rearrangement or modulation of the periodicity are induced, in order to reduce the surface energy. From this standpoint, structures that do not undergo chemical bond breaking on the surface, such as molecular crystals or layered materials, are considered to be stable. In fact, in contrast with inorganic crystals, most of the other materials actually exhibit less change in the surface structure.

However, recently, using scanning tunneling microscopy (STM) and related techniques, the existence of marked structural modulations introduced by surface relaxation/reconstruction has been revealed on the surface of bis(ethylenedithio)tetrathiafulvalene (BEDT-TTF) based low-dimensional organic conductors.[5–14]

Figure 1 shows the crystal structure of β-(BEDT-TTF)$_2$PF$_6$,[15,16] an organic conductor recognized one-dimensional along the side-by-side (transverse) array, in the direction of the *c* axis. In the crystal, BEDT-TTF and PF$_6$ layers are alternately stacked along the *b* axis, and each of them appears as the top layer of the surface on the *a*-*c* plane. In STM images, contrast to the crystal structure, twofold periodic modulation along the crystal *a* axis was observed for both surfaces.[5]

In the case of the surface terminated by PF$_6$ molecules, drastic change occurs, namely, PF$_6$ molecular rows are alternately missing along the crystal *a* axis [Fig. 1(b)].[5] On the other hand, for the surface with BEDT-TTF molecules, the unit cell of the BEDT-TTF layer consists of four BEDT-TTF molecules, which form two dimmers [*A*-*B* and *C*-*D* in Fig. 1(b)]. If the surface retains the ideal crystal structure, molecules *A* and *C* should be observed with the same shape and brightness in the STM image of the crystal *a*-*c* plane because they have the same structure and are the same distance from the surface. However, alternately modulated molecular rows appear.

The origin of the observed surface structures was explained by a mechanism similar to that which is used to understand the surface structures of inorganic materials consisting of atomic elements, such as Si(100) and GaAs(100).[1–3] Through the transfer of 0.5 electrons from each BEDT-TTF molecules to anion layers, BEDT-TTF and anion layers become conductive and insulating, respectively. However, in the surface top layer, one side layer does not exist, and charge transfer is half and incomplete similar to the semiconductor surfaces.

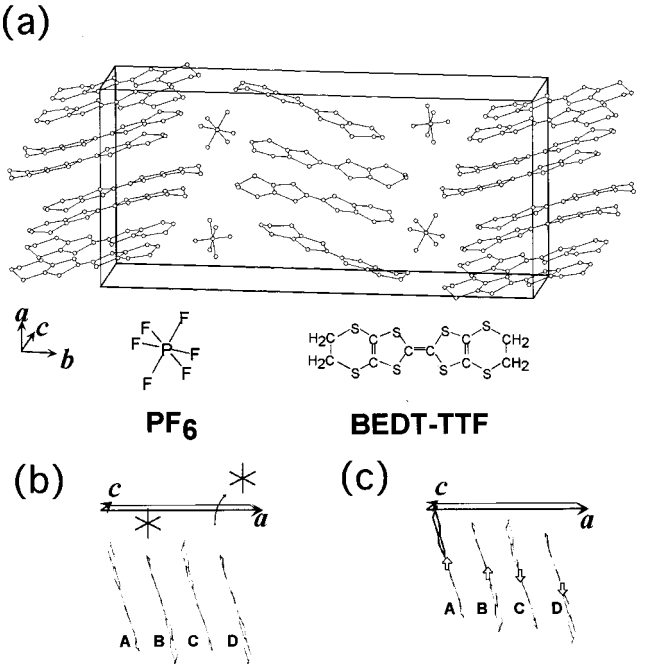

FIG. 1. Schematic structure of β-(BEDT-TTF)$_2$PF$_6$ crystal (a), and the structural models for the surface top layer terminated by (b) PF$_6$ and (c) BEDT-TTF molecules.

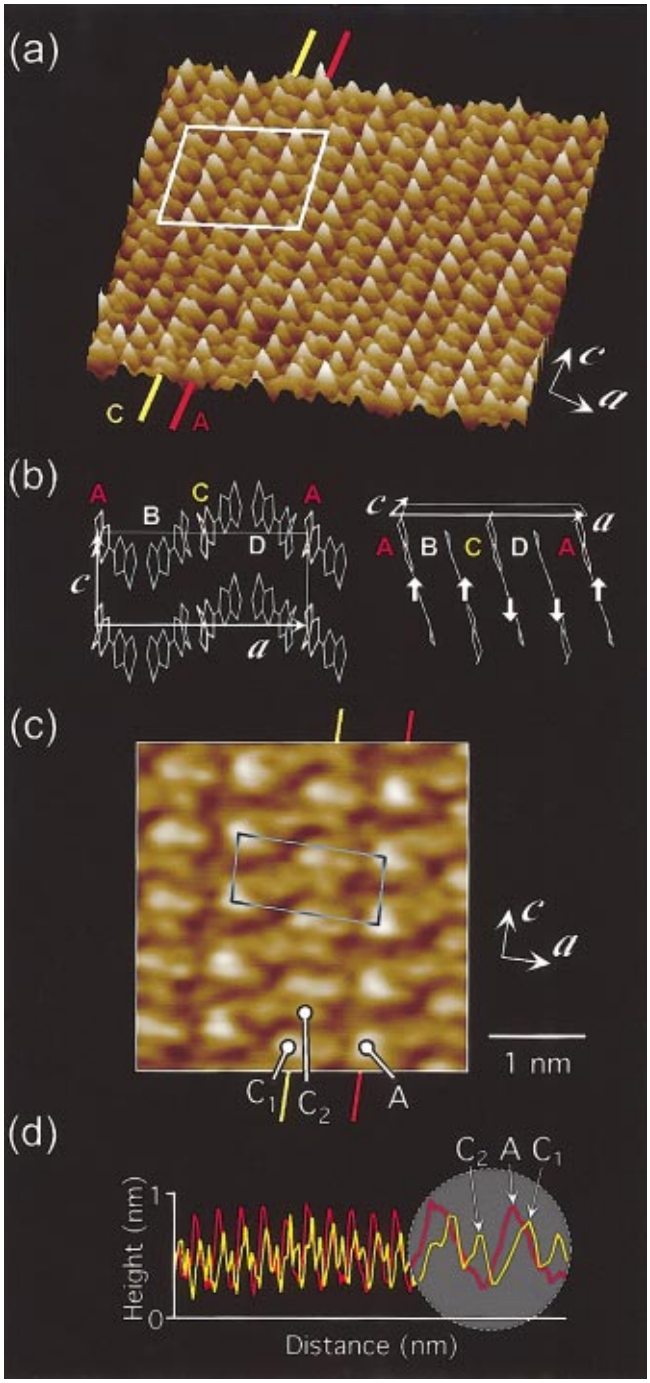

FIG. 2. (Color) (a) Typical STM image of β-(BEDT-TTF)$_2$PF$_6$. (b) Top and side views of the molecular arrangement in a unit cell. (c) Magnification of the squared area in (a). (d) Cross sections along the red and yellow lines in (a).

In As-rich GaAs(100) surface, As dimmer rows are orderly missing which improves the charge transfer in the surface layers. Assuming a similar mechanism for the surface terminated by PF_6 molecules, when half of the PF_6 molecules are removed [Fig. 1(b)], the charge is exactly balanced within the surface layer, resulting in stable surface.[5] On the other hand, in the case of the surface terminated by BEDT-TTF molecules, since the BEDT-TTF molecules strongly interact with the adjacent BEDT-TTF molecules, they are not

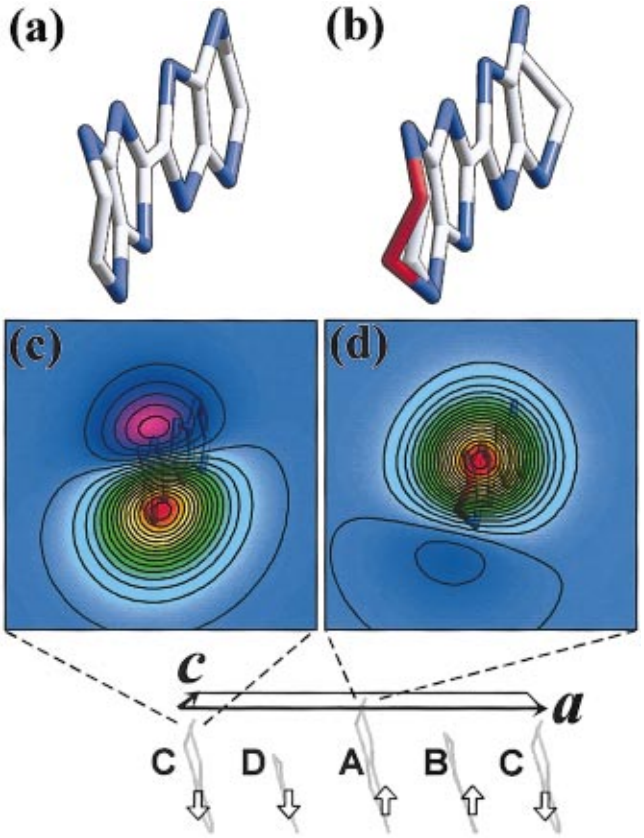

FIG. 3. (Color) Structure of the molecule in the crystal projected onto the *a*-*c* plane (a) and the relaxed molecular structure derived from the calculation (b). Ethylene group at the one end of the molecule is colored red. (c) and (d) are the spatial distributions of HOMO for the structures of two types corresponding to (a) and (b).

desorbed and only structural modulation occurs such as the buckling of Si dimmers. Namely, dimmers *A*-*B* and *C*-*D* in a unit cell are pulled toward the surface and inside, respectively [Fig. 1(c)].[5]

The basic mechanism for the surface relaxation has been considered to be established. However, since the elements are molecules in the case of molecular crystals, further change regarding the elemental molecules is expected to occur. Namely, structure of the elemental molecules is expected to play a role in the formation of crystals or surface structures. In fact, we found a unique mechanism operating in the surface relaxation process of molecular crystals of BEDT-TTF compounds.

Figure 2(a) shows a three-dimensional view of the typical STM image acquired over the *a*-*c* plane of β-(BEDT-TTF)$_2$PF$_6$. For comparison, top and side views of the molecular arrangement is shown in Fig. 2(b). STM measurements were performed in the topographic mode over the two-dimensional (2D) BEDT-TTF molecular layer terminating the surface, under ambient conditions using a Pt/Ir tip. The conduction band of cation salts consists of the highest-occupied molecular orbital (HOMO), from which the other energy levels are separated enough. In fact, no bias dependence was observed, reflecting the fact that no other molecular orbital contributes to the energy levels near the Fermi level, except for the HOMO.

Dimensions of the surface unit cell estimated from the STM image are $a=0.65$ nm and $c=1.50$ nm, and are in good agreement with the lattice parameters determined by x-ray diffraction, $a=0.67$ nm and $c=1.50$ nm. The molecular rows aligned in the direction of the most conductive axis, the c axis, are alternately modulated in bright and dark [indicated by red and yellow lines in Fig. 2(a)], as previously observed by STM/AFM.[3] The measured height difference of the two dimers is 0.1 nm in the direction perpendicular to the surface, and consequently, the 1D feature along the c axis appears in the STM/AFM images. This change is the intermolecular symmetry breaking due to the surface relaxation as mentioned above [Fig. 1(c)].[5]

In order to analyze the observed difference in the molecular images of the two types of molecular rows in more detail, a magnified image of the squared area in Fig. 2(a) and cross sections along the two adjacent types of dimmer rows indicated by yellow and red lines in Fig. 2(a) are shown in Figs. 2(c) and 2(d), respectively. As expected, there exists an additional difference. As the most noteworthy point, the brighter molecule, molecule *A*, has only one protrusion, although two protrusions exist at the darker molecule, molecule *C* (protrusions C_1 and C_2). This difference is clearly seen in the cross section in Fig. 2(d).

In previous studies, two different calculations have been reported to interpret the STM images of the BEDT-TTF compounds. One is the tight-binding calculation, concluding that the surface HOMO density of the BEDT-TTF compounds is dominated by the topmost hydrogen-related orbital,[10–12] and the other focuses on the contribution of the sulfur orbital to the HOMO.[13] However, characteristics of the newly confirmed modulation, appearance of a single or a pair of two protrusions from a BEDT-TTF molecule, cannot be reproduced by either of these two calculations.

A possible mechanism explaining the observed characteristics in the STM image is to consider the intramolecular relaxation on the surface. In fact, in the crystal, face-to-face BEDT-TTF molecules are strongly dimerized,[15] and the molecules are distorted from their relaxed structure as will be discussed in detail later. The increase in the energy due to the deformation is estimated to be 4% per molecule, and the molecular structure in the crystal is stabilized by the existence of the anion layers sandwiching the BEDT-TTF layer. Therefore, occurrence of the intramolecular relaxation on the surface due to the missing of the anion layer is mostly probable.

In order to clarify the molecular structure on the surface, we calculated the spatial distribution of the BEDT-TTF HOMO using density-functional theory (DFT) with the generalized gradient approximation (GGA) of Perdew and Wang (PW91). To make a comparison between the STM results and the calculation, two types of molecular structures were examined. One is the structure appearing in the crystal that is derived from the x-ray diffraction measurement, which was used in the previous calculations to reproduce the STM images. The other is the relaxed molecular structure calculated by optimization of the molecular structure. In our calculation, we took into account the sulfur $3d$ orbital, which was not considered in earlier calculations despite the fact that it must make a great contribution to the side-by-side structure of the HOMO.[15] As shown later, spatial distribution of the $3d$ orbital plays an important role to reproduce the obtained STM images.

Figures 3(a) and 3(b) illustrate the molecular structure in the crystal projected onto the *a*-*c* plane and the relaxed molecular structure derived from the calculation, respectively. As indicated by the part colored red in Fig. 3(b), the main difference appears around the topmost ethylene group ($—CH_2—CH_2—$), which is considerably relaxed in the optimized structure. In the crystal, the four carbon orbitals related to the ethylene group exhibit an energy shift toward the lower binding energy ($\sim$1 eV for the C $1s$ orbital) as compared with the other carbon orbitals. However, the sulfur-related orbitals produce less difference between these structures even in the HOMO. This result indicates that the influence of crystallization is concentrated in the four carbon atoms forming the ethylene groups.

Spatial distributions of the HOMO for the two types of molecule are shown in Figs. 3(c) and 3(d). The contour plots are 0.5 nm away from the topmost hydrogen atom and are illustrated together with the molecular frames shown in Figs. 3(a) and 3(b), respectively. Despite the change in the density of state with the distance from the surface, the general features of the plots were less dependent on the distance. As shown in these figures, the two types of molecular structure yield completely different distributions of the HOMO.

As shown in Fig. 3(c), the surface HOMO density for the molecule in the crystal has two distinct peaks divided by a node. The distance between the two peaks is $\sim$0.40 nm, which is in good agreement with the experimental value appearing in Fig. 2(c) as molecule C (distance between C_1 and C_2), 0.41 nm.

The origin of the upper peak of the HOMO density is the p- and d-π electrons from the sulfur just below the higher density position. Another peak located in the lower part includes the π electron of the C—C bond. The appearance of the π characteristic in addition to the σ bond suggests the existence of high strain in the ethylene group. As has been shown, the sulfur-related orbitals account for the HOMO density, which is higher than in the previous results. The appearance of the sulfur component in this case is explained by the introduction of $S\,3d$ into the calculation, because $S\,3d$ in BEDT-TTF has a large distribution in the direction normal to the surface.

On the other hand, for the optimized molecule, only one large peak dominates the HOMO density [Fig. 3(d)], unlike to the molecule in the crystal shown in Fig. 3(c). The result is in good agreement with the STM image of molecule *A* in Fig. 2(c). The origin of the dominant peak appearing over the top of the molecule is the same component of the sulfur orbital referred to in Fig. 3(c). The low density peak located in the lower part is not from the p-π-like orbital of the ethylene group but from the orbital of another sulfur near the surface plane. Structural optimization of the molecule results in the disappearance of the π-like orbital of the ethylene group, which dominated a considerable part of Fig. 3(c). Therefore, the STM image of the BEDT-TTF compounds is dominantly characterized by the distribution of the sulfur-

related orbital near the surface, and the additional component appears as protrusion depending on the local strain in the ethylene group.

On the basis of the comparison between Fig. 2(c) and Fig. 3, as described above, molecules *C* and *A* in Fig. 2(c) can be attributed to molecules which have a molecular structure appearing in the crystal [Fig. 3(c)] and a relaxed molecular structure [Fig. 3(d)], respectively. The obtained result indicates that the structural relaxation of the elemental molecules is not negligible during the formation of the surface structures of BEDT-TTF compounds.

The characteristic features observed for β-(BEDT-TTF)$_2$PF$_6$ have not been pointed out until now. However, they can be seen in the STM images of previous works on other BEDT-TTF-based compounds with the 1D characteristic, such as α-(BEDT-TTF)$_2$I$_3$ (Ref. 10) and (BEDT-TTF)$_2$TlHg(NCS)$_4$.[11] Their STM images also show the two types of molecular images: a single large protrusion and a pair of two protrusions.

Since the deformation energy of the BEDT-TTF molecules is balanced by the intermolecular interaction, intermolecular and intramolecular symmetry breaking must have a strong relationship. In most of the BEDT-TTF compounds, BEDT-TTF molecules are stacked in a face-to-face structure forming a molecular column, as shown in Fig. 1. It is due to the anisotropic molecular interaction. In the case of the BEDT-TTF compounds with 1D-like structure, the conductivity in the BEDT-TTF compounds is characterized by strong π-π interaction in the molecular column. Therefore, the stronger anisotropic interactions between neighboring molecules may suppress the flexible relaxation of the surface structure, and the structural relaxation is considered to be restricted by the column structure. Further study is needed to make a complete understanding of the relationship between intermolecular and intramolecular relaxations.

In conclusion, we found a unique mechanism operating in the surface relaxation process of BEDT-TTF-based molecular crystals. In addition to the intermolecular symmetry breaking which is generally observed during the surface relaxation of atomic crystals, the intramolecular relaxation was confirmed to play a role in the formation of the surface structure. Since the physical properties of materials depend on the characteristics of the crystal elements, this mechanism is fundamentally important and expected to aid in designing and developing multifunctional molecular devices in the future.

*Present address: Fundamental Research Laboratories, NEC Corporation Tsukuba, 305-8501, Japan.

†Corresponding author. Email address: hidemi@ims.tsukuba.ac.jp http://dora.ims.tsukuba.ac.jp

[1] M. Tsukada and T. Hoshino, J. Phys. Soc. Jpn. **51**, 2562 (1982).

[2] K. W. Haberern and M. D. Pashley, Phys. Rev. B **41**, 3226 (1990).

[3] R. M. Tromp, R. J. Hamers, and J. E. Bemuth, Phys. Rev. Lett. **55**, 1303 (1985).

[4] M. D. Pashley *et al.*, Phys. Rev. Lett. **60**, 2176 (1988); H. Shigekawa *et al.*, Appl. Phys. Lett. **65**, 607 (1994).

[5] M. Ishida, K. Hata, T. Mori, and H. Shigekawa, Phys. Rev. B **55**, 6773 (1997); H. Shigekawa *et al.*, *ibid.* **52**, 16 361 (1995); M. Ishida, T. Mori, and H. Shigekawa, Jpn. J. Appl. Phys., Part 1 **39**, 3823 (2000); Phys. Rev. Lett. **83**, 596 (1999).

[6] M. Yoshimura *et al.*, Phys. Rev. B **44**, 1970 (1991).

[7] R. Fainchtein *et al.*, Science **256**, 1012 (1992).

[8] S. Yoon *et al.*, Phys. Rev. B **47**, 4802 (1993).

[9] M. Ishida, T. Mori, and H. Shigekawa, Surf. Sci. **433–435**, 147 (1999).

[10] S. N. Magonov *et al.*, Synth. Met. **62**, 83 (1994).

[11] S. N. Magonov *et al.*, J. Phys. Chem. **97**, 9170 (1993).

[12] S. N. Magonov and M.-H. Whangbo, Adv. Magn. Reson. **6**, 355 (1994).

[13] M. Yoshimura *et al.*, Phys. Rev. B **43**, 13 590 (1991).

[14] K. Hashimoto *et al.*, Jpn. J. Appl. Phys. **38**, L464 (1999).

[15] T. Mori *et al.*, Solid State Commun. **53**, 627 (1985).

[16] H. Kobayashi *et al.*, Chem. Lett. **1983**, 581 (1983).